

CONF-8510173--45

IRRADIATION EFFECTS IN LOW-ALLOY REACTOR PRESSURE VESSEL STEELS
(HEAVY-SECTION STEEL TECHNOLOGY PROGRAM SERIES 4 AND 5)*

J. J. McGowan, R. K. Nanstad, K. R. Thoms,† and B. H. Menke‡

Metals and Ceramics Division
OAK RIDGE NATIONAL LABORATORY
Oak Ridge, Tennessee 37831

CONF-8510173--45
TI86 004768

INTRODUCTION

Numerous studies of the effects of impurities and fast neutron irradiation on fracture toughness of nuclear reactor pressure vessel materials (plates, forgings, and welds) have been reported in the literature.¹⁻⁹ Most such studies have included a minimum number of tests for each material and/or combination of irradiation parameters. Statistical analysis of neutron irradiation effects has been possible only by using a large body of data representing a variety of materials and neutron exposure conditions. However, such analytical methods do not address the question of accuracy of each datum in the large set, or the accuracy and reliability of results from a single small data set such as might be obtained in a nuclear reactor pressure vessel surveillance study. The present studies address this question by multiple testing at two laboratories of typical nuclear pressure vessel materials (both irradiated and unirradiated) and statistical analyses of the test results. Multiple tests are conducted at each of several test temperatures for each material, standard deviations are determined, and results from the two laboratories are compared.

The Fourth Heavy-Section Steel Technology (HSST) Irradiation Series, almost completed, was aimed at elastic-plastic and fully plastic fracture toughness of low-copper weldments ("current practice welds"). A typical nuclear pressure vessel plate steel was included for statistical purposes.

The Fifth HSST Irradiation Series, now in progress, is aimed at determining the shape of the K_{IR} curve after significant radiation-induced shift of the transition temperatures. This series includes irradiated test specimens of thicknesses up to 100 mm and weldment compositions typical of early nuclear power reactor pressure vessel welds.

These two series will be discussed separately.

*Research sponsored by the Office of Nuclear Regulatory Research, U.S. Nuclear Regulatory Commission, under Interagency Agreements DOE 40-551-75 and 40-552-75 with the U.S. Department of Energy under contract DE-AC05-84OR21400 with Martin Marietta Energy Systems, Inc.

†Engineering Technology Division, Oak Ridge National Laboratory.

‡Materials Engineering Associates, Lanham, Maryland.

MASTER

PRODUCTION OF THIS DOCUMENT IS UNLIMITED

By acceptance of this article, the publisher or recipient acknowledges the U.S. Government's right to retain a nonexclusive, royalty-free license in and to any copyright covering the article.

JSW

FOURTH HSST IRRADIATION SERIES

This irradiation program was conducted on four submerged-arc welds and one of A533 grade B class 1 pressure vessel steel. The welds were made by commercial vendors using current welding practices and contained relatively low copper contents. The target fast neutron fluence was 2×10^{23} neutrons/m² (>1 MeV) and the irradiation temperature was 288°C (550°F). Charpy V-notch, tensile, and fracture toughness tests (ITCS specimens) were conducted. Sufficient numbers of specimens were included in the irradiations to permit statistical analyses of the results.

MATERIALS

The plate material was from a 305-mm-thick plate of ASTM A533 grade B class 1 manganese-molybdenum-nickel steel produced by Lukens Steel Company for the HSST Program.¹⁰ This plate material was designated HSST plate 02 and portions of it have been used in many investigations. All test specimens were prepared in the transverse (TL) orientation.

All four submerged-arc weldments were made in ASTM A533 grade B class 1 plate. Two of the submerged-arc weldments were supplied by the Electric Power Research Institute (EPRI) and had been fabricated by Combustion Engineering, Inc. HSST weld 68W was produced as a 178-mm-thick submerged-arc welding using Linde 0091 flux and 4.8-mm-diam MIL-B-4 (low copper and phosphorus) wire and was designated "CGS" in EPRI studies.¹¹ HSST weld 69W was produced as a 300-mm-thick submerged-arc weldment using Linde 0091 flux and 4.8-mm-diam MIL-B-4 wire and was designated "CHS" in EPRI studies.¹¹ Both welds were postweld heat treated 25 h at 621°C. The other two welds were supplied by Babcock and Wilcox Company.¹² Both welds were produced as 174-mm-thick submerged-arc weldments using Mn-Mo-Ni (SFA-5.23EF2N) filler wire. HSST weld 70W was fabricated using Linde 0124 flux and HSST weld 71W was fabricated using Linde 0080 flux. Both welds were postweld heat treated 48 h at 607°C.

All test specimens were prepared with longitudinal axes perpendicular to the weld centerline and crack propagation direction parallel to the surface. The four weldments are considered "current practice" and are of low or medium low-copper content. Two of the welds (EPRI material) also had low-nickel contents. Chemical compositions of the five materials are presented in Table 1.

MATERIAL IRRADIATION

All irradiations were conducted at two faces of the Bulk Shielding Reactor (BSR) at Oak Ridge National Laboratory (ORNL), a 2-MW pool-type reactor. Thermal shields of 42.5-mm-thick stainless steel were used between the reactor core and the specimen capsules to reduce gamma heating in the irradiation capsules. Each capsule contained 60 ITCS fracture toughness specimens, 80 to 90 Charpy V-notch impact test specimens, and 10 to 20 tensile test specimens in an arrangement shown in Fig. 1.

Table 1. Chemical compositions of plate and submerged-arc welds

Material	Composition, wt %									
	C	Mn	P	S	Si	Cr	Ni	Mo	Cu	V
Plate, A533 grade B class 1 (HSST-02)	0.23	1.55	0.009	0.014	0.20	0.04	0.67	0.53	0.14	0.003
Weld HSST-68W, Linde 3091 flux	0.15	1.38	0.008	0.009	0.16	0.04	0.13	0.60	0.04	0.007
Weld HSST-69W, Linde 0091 flux	0.14	1.19	0.010	0.009	0.19	0.09	0.10	0.54	0.12	0.005
Weld HSST-70W, Linde 0124 flux	0.10	1.48	0.011	0.011	0.44	0.13	0.63	0.47	0.056	0.004
Weld HSST-71W, Linde 0080 flux	0.124	1.58	0.011	0.011	0.54	0.12	0.63	0.45	0.046	0.005

Specimen temperatures during irradiation were controlled by a combination of electrical heaters and controlled sweep gas composition (helium and nitrogen). Specimen temperatures during irradiation were controlled at $288 \pm 5^\circ\text{C}$. Irradiation times for the capsules ranged from 4300 to 5400 h.

Complete spatial maps of damage exposure parameter values were determined for each capsule. The dosimetry in the capsules consisted of multiple foil sets and gradient wires. The dosimetry and spectral adjustment procedures are completely presented elsewhere.¹³⁻¹⁴ The values of fluences greater than 1 MeV, 0.1 MeV, and displacements per atom (dpa) were determined for each specimen. Uncertainties for the damage exposure parameters were less than 8% (standard deviation).

TEST PROCEDURES

The Charpy V-notch impact testing was apportioned between Materials Engineering Associates (MEA), Lanham, Maryland, and ORNL, Oak Ridge, Tennessee, such that both laboratories tested equivalent specimens insofar as possible.

The impact testing machines at both laboratories were calibrated in conformance with ASTM Standard Method E23, including proof tests using "standardized specimens." Nonlinear least-squares procedures¹⁵ were used to determine the best hyperbolic tangent fit to the data:

$$E = A * \{1 + \tanh[B * (T-C)]\}/2. \quad (1)$$

where

- E = fracture energy, J,
- T = test temperature, °C,
- A, B, C = parameters determined in the fitting process.

REPRODUCED FROM
BEST AVAILABLE COPY

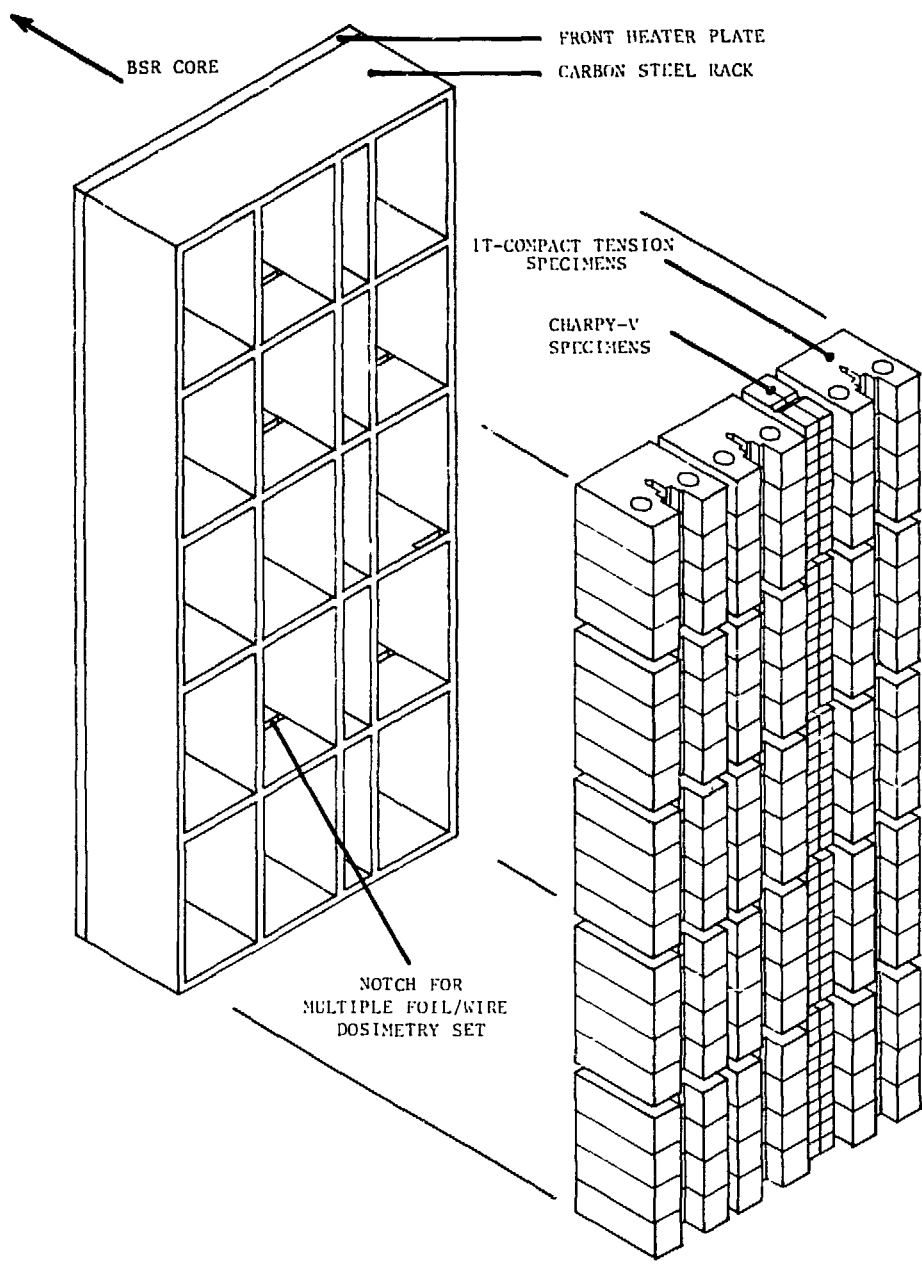


Fig. 1. Fourth HSST Irradiation Series capsule specimen rack assembly.

The transition temperature is calculated by solving Eq. (1) for the temperature at 41 J. A positive transition temperature shift (ΔT) is an increase in transition temperature from the unirradiated to irradiated state.

The upper shelf energy is equal to the curve fit parameter A in Eq. (1). A positive upper-shelf energy change (ΔE) is an increase in upper-shelf energy from the unirradiated to the irradiated state.

An attempt was made to analyze the radiation-induced changes as a power law function of neutron fluence. However, with the maximum neutron fluence range of only $\pm 50\%$, the scatter of the data was such that a reliable analysis could be made only for plate O2. Each data point in the transition range for plate O2 was adjusted on the temperature scale to correct each specimen fluence to the mean value (2×10^{23} neutrons/m², $E > 1$ MeV).

Testing of compact specimens (CS) was performed by the single specimen compliance (SSC) technique with each laboratory testing approximately half the specimens. All compact specimens designated for upper-shelf testing were side-grooved on each side by 10% of the specimen thickness. The SSC technique provides a method to determine the amount of specimen crack extension by means of small unloadings (<15% of maximum load) conducted at regular intervals throughout the test.

Values of the J-integral were calculated using the modified version of the J-integral, known as J_M , as proposed by Ernst.¹⁶ Deformation theory J (J_D) is the formulation of the J-integral specified for use in the ASTM Standard Test for J_{IC} , a measure of fracture toughness, E813-81, and in the tentative ASTM J-integral resistance (J-R) curve test procedure.¹⁷ Modified J (J_M) was used in this program because Ernst has shown it to be more specimen-size independent when the crack extension exceeds the J-controlled crack growth regime.

A typical R curve produced with the SSC technique is illustrated in Fig. 2. The R curve format of Fig. 2 is in accordance with that of ASTM Standard E813, i.e., J_{IC} , the initiation elastic-plastic fracture toughness, is defined by the intersection with the blunting line of the linear regression fit to the data between the 0.15- and 1.5-mm exclusion lines. The use of linear least-squares fit stems from the multispecimen nature of ASTM E813 where a minimum of only four data points are required. Thus, with only a few data points, the nonlinear nature of the R curve cannot be evaluated. For this study, the procedure proposed by Loss et al.,¹⁸⁻¹⁹ was used whereby a power law, $J = C(\Delta a)^N$, is fit to the data between the 0.15- and 1.5-mm exclusion lines with the constants C and N chosen to optimize the curve fit. The initiation fracture toughness, J_{IC} , is defined with this procedure as the intersection of the power law R curve with the 0.15-mm exclusion line as indicated in Fig. 2. J_{IC} , as defined by the two methods, is nearly identical for nuclear grade pressure vessel steels. In addition to more closely describing the nonlinear behavior of the R curve, the power law J_{IC} definition provides a consistent means for determining the initiation toughness when fast fracture, i.e., brittle fracture by a cleavage micromode, occurs prior to development of a full R curve. To address this cleavage phenomenon, the power law method classifies the R curve into three types: types A, B, and C. With type A, failure occurs before the slow ductile crack extension is sufficient to cross the 0.15-mm exclusion line. In this case, J_{IC} is taken as the value

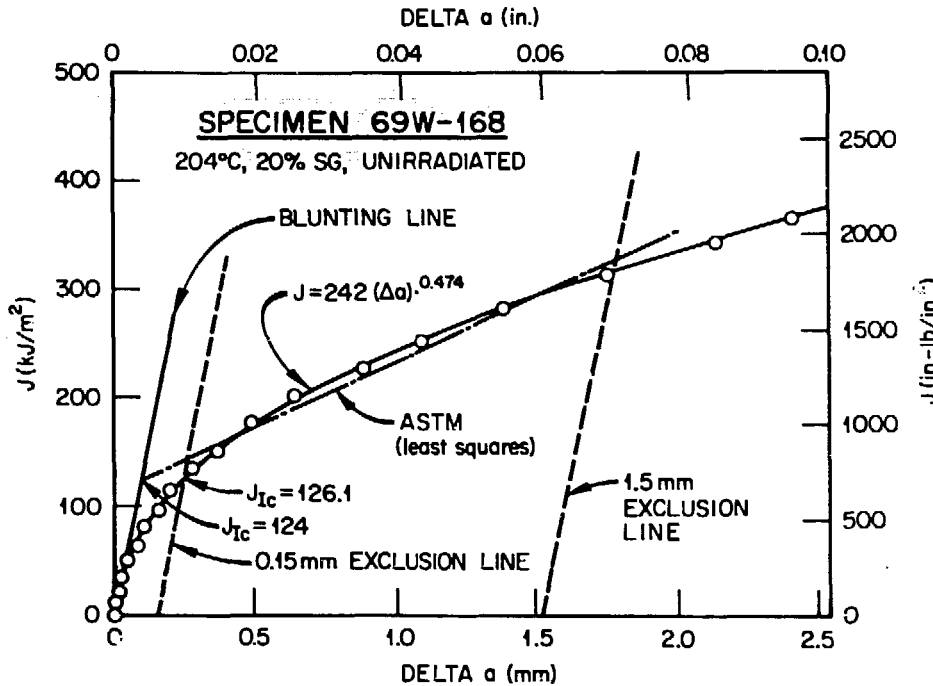


Fig. 2. Power law representation of the J-R curve using the SSC test technique and comparison with the ASTM E813 procedure.

of J_M at failure. Type B covers cases where testing was terminated by fast fracture after ductile crack extension exceeded the 0.15-mm exclusion line, but prior to reaching the 1.5-mm exclusion line, whereas type C covers cases where the R curve extends beyond the 1.5-mm exclusion line. In these cases, a power law is fit to the available data and J_{Ic} is taken as the intersection of the fit with the 0.15-mm exclusion line.

Another effect resulting from the nonlinear nature of the R curve is that the tearing modulus is not constant as was originally envisioned by ASTM E813. For comparison purposes and consistency with ASTM E813, a single value for the tearing modulus (T_{avg}) can be computed from the power law equation for type C resistance curves. The tearing modulus is defined as

$$T = \frac{E}{\sigma_f^2} \frac{dJ}{da}, \quad (2)$$

where $\sigma_f = (\text{yield stress} + \text{ultimate stress})/2$. To obtain an average value for the slope of the power law R curve, the power law equation is fit in closed form with a linear regression of the form $J = J_0 + (dJ/da)\Delta a$ to that part of

the curve lying between the exclusion lines. This technique is directly analogous to the E813 method of fitting a linear line to the discrete data points. However, fitting the power law equation has the effect of including an infinite number of points. Little difference in magnitude is observed between the values of T obtained by the two techniques.

The power law and E813 methodologies produce similar results in regions covered by the E813 standard.²⁰⁻²¹ The procedure is to convert the elastic-plastic J_{IC} power law initiation toughness to a quasielastic K_{JC} value using the following relationship:

$$K_{JC} = (EJ_{IC})^{0.5} , \quad (3)$$

where $E(\text{GPa}) = 207.2 - 0.057 T(^{\circ}\text{C})$.

ASTM Standard E813 gives an equation for converting J_{IC} to K_{JC} , which incorporates a plane-strain term. Equation (3) is identical to the E813 equation, but with the plane-strain term removed. This term was removed because in this program specimens tested in the upper transition region and those tested on the upper shelf experienced net section yielding. Such behavior is closer to plane stress than it is to plane strain. In the lower transition region, however, the specimen through-thickness constraint is greater and more nearly plane strain. Thus, it is unclear just where one should use the E813 equation. Since most of the data generated in this study were more nearly plane stress and, for consistency of presentation, all K_{JC} values were calculated using Eq. (3).

At toughness levels too great to allow measurement of a valid K_{IC} with a small specimen, K_{JC} values can be determined as stated above; however, these data tend to be of greater magnitude than that which would be obtained with a larger specimen capable of measuring the linear elastic toughness level by E399 criteria. A similar observation was made by Irwin²² in that the plane stress fracture toughness (K_c) overestimates K_{IC} . Irwin developed an empirical relationship from which K_{IC} could be estimated once K_c was known. Recently, Merkle²³ has shown that reasonable estimates of K_{IC} can be determined using K_{JC} as a substitute for K_c . In this study, K_{JC} values in the ductile-to-brittle transition region were corrected to $K_{\beta C}$ using the Irwin-Merkle β_{IC} correction to provide another means of determining the shift to higher temperature of the ductile-to-brittle transition caused by irradiation.

RESULTS — FRACTURE TOUGHNESS TESTS

All side-grooved specimen J-R curves obtained in this study were valid by ASTM E813 criteria. The agreement between MEA and ORNL data, both in the transition and upper-shelf regimes, is excellent.

The fracture toughness behavior for two materials in terms of the quasi-elastic parameter K_{JC} is illustrated in Figs. 3 and 4. In these figures, the solid line trend curves are the result of regression curves fit to all data points. On the upper shelf, a linear regression was used and in the transition the data were fit with an exponential of the form $K_{JC} = C + A[\exp(B \cdot \text{temperature})]$ with the constants A, B, and C chosen to optimize the fit. All shifts in transition temperature were calculated using the exponential curve fit equations.

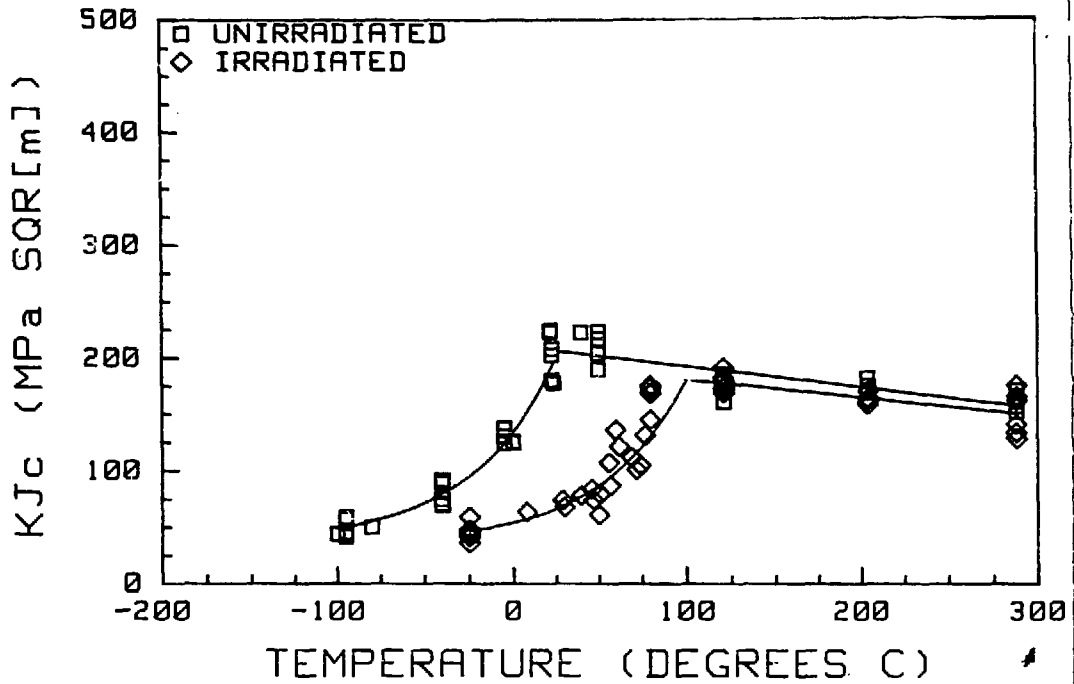


Fig. 3. Variation of K_{Jc} with temperature and irradiation of HSST plate 02.

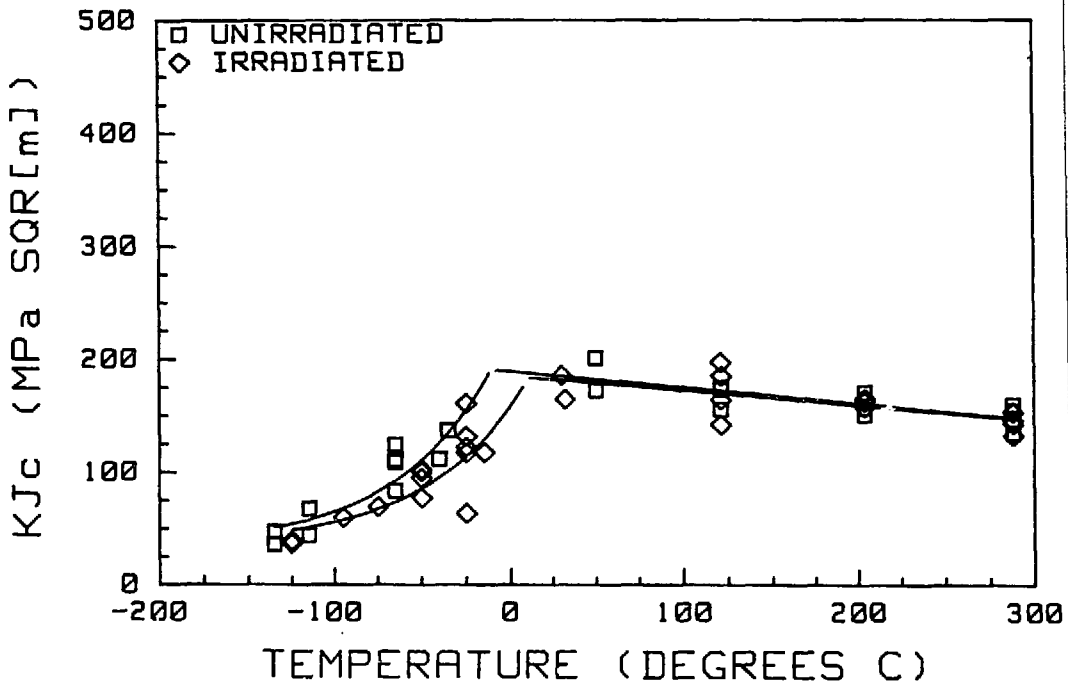


Fig. 4. Variation of K_{Jc} with temperature and irradiation of HSST weld 70W.

Data for plate 02 material are depicted in Fig. 3. This material had the highest levels of both copper (0.14%) and nickel (0.67%) and the K_{Jc} data indicate the greatest shift in the transition temperature. There is not, however, a corresponding large change in upper-shelf toughness. Data scatter is relatively low for this material, as would be expected in a homogeneous reference material such as plate 02.

Figure 4 illustrates the behavior indicated for weld 70W. This weld had a low copper level (0.046%), but a similar nickel level (0.63%). The transition shift is relatively small compared with that for plate 02, and the upper shelf change is not significant.

The fracture toughness behavior in terms of the thickness-corrected parameter $K_{\beta c}$ is shown in Figs. 5 and 6. In these figures the solid line trend curves are the result of regression curves fit to all data points. (Only those specimens that cleaved are used here.) The data are fit with an exponential of the same form as used for the K_{Jc} data. Data for plate 02 are depicted in Fig. 5, while Fig. 6 illustrates the behavior indicated for weld 70W.

The effect of temperature and irradiation on tearing modulus is shown in Figs. 7 and 8. All data were fit with a linear regression. In general T_{avg} decreases with increasing temperature and with irradiation. Data for plate 02 are depicted in Fig. 7. This material had the highest values of copper and nickel, and the greatest drop in tearing modulus with irradiation. Data for weld 70W is shown in Fig. 8. This material had a lower value of copper and similar nickel than plate 02 with a corresponding smaller drop in tearing modulus as a consequence of irradiation.

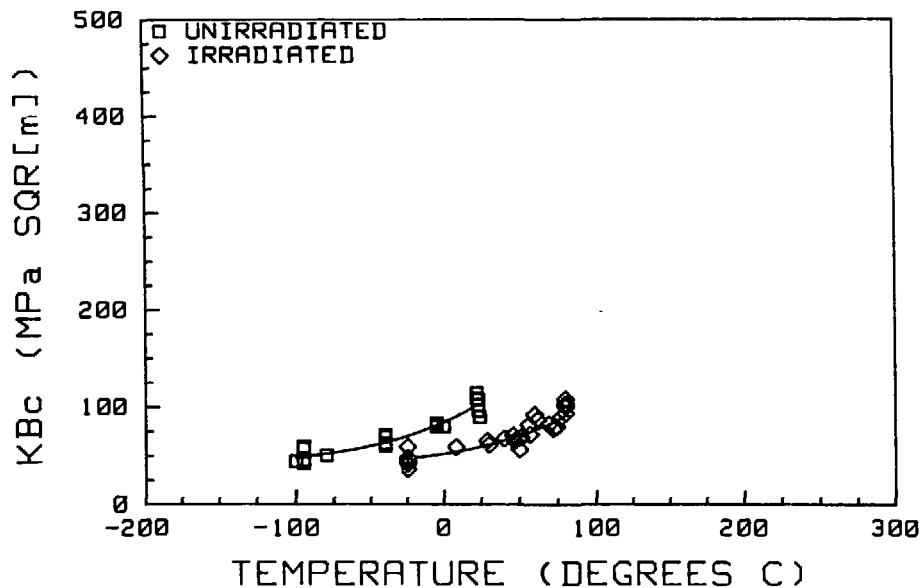


Fig. 5. Variation of $K_{\beta c}$ with temperature and irradiation of HSST plate 02.

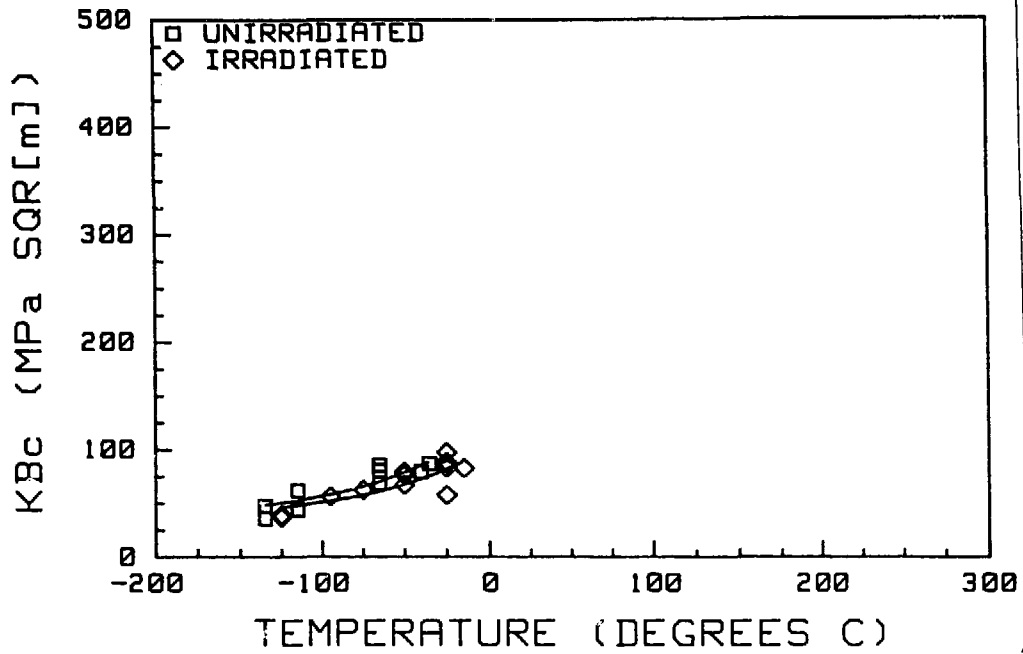


Fig. 6. Variation of $K_{\beta c}$ with temperature and irradiation of HSST weld 70W.

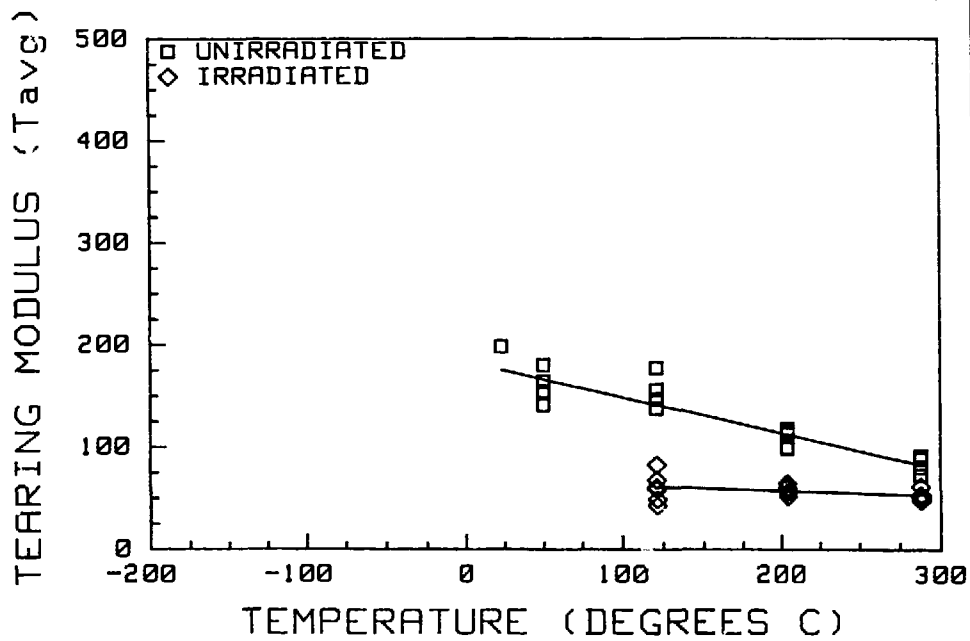


Fig. 7. Variation of tearing modulus with temperature and irradiation of HSST plate 02.

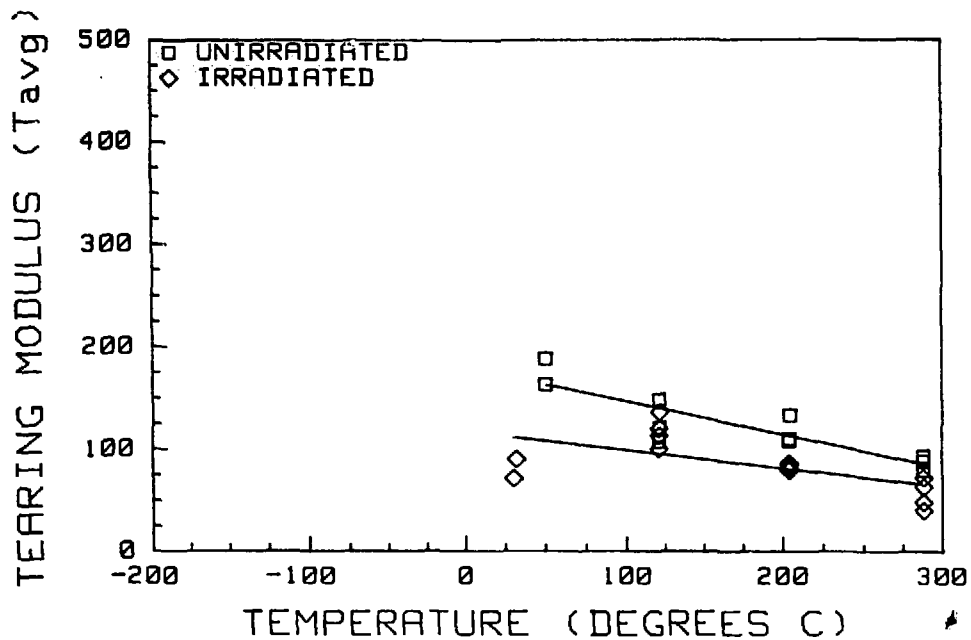


Fig. 8. Variation of tearing modulus with temperature and irradiation of HSST weld 70W.

The results of this irradiation effects study are summarized in Table 2. (The tensile and Charpy V-notch results have been presented earlier in refs. 24 and 25.) The CVN shift was indexed at 41 J and K_{Jc} was indexed at 125 $\text{MPa}\sqrt{\text{m}}$. $K_{\beta c}$ was indexed at 90 $\text{MPa}\sqrt{\text{m}}$ for all five materials. This $K_{\beta c}$ level roughly corresponds (for a 25-mm-thick compact specimen) to the β_{Ic} -corrected 125 $\text{MPa}\sqrt{\text{m}}$ K_{Jc} index for all five materials. Comparison of the CVN shift with K_{Jc} , and $K_{\beta c}$ indexed at 90 $\text{MPa}\sqrt{\text{m}}$ give similar results since the unirradiated and irradiated K_{Jc} and $K_{\beta c}$ transition curves are essentially parallel.

It is clear that the transition temperature shift is reduced by decreasing both the copper and the nickel content. Reducing either one separately does not produce as substantial a change in the shift as reducing both. Only the welds can be compared directly. The highest shift is evidenced by the data from weld 69W with the highest copper and lowest nickel, thus indicating that copper alone has a substantial effect. However, increased nickel with lowered copper (welds 70W and 71W) also produces a substantial but lesser shift. The lowest shift was produced in weld 68W where the percentage of both elements was reduced. It must also be noted that the silicon contents of welds 70W and 71W were more than double those for the other welds and the average fluences are greater for 70W and 71W than for 68W and 69W. Final analyses will incorporate a method of fluence normalization to allow for better comparison of results. Although the magnitude of the transition temperature shift varies somewhat for each indicator, all three support these observations.

Table 2. Summary of material properties after irradiation

Material	Mean Fluence, $n/m^2 \times 10^{23}$ (>1 MeV)	Yield strength increase ^a (%)	Transition temperature increase (°C)			Upper-shelf change (%)		Tearing modulus change ^a (%)	dJ/da change ^a (%)
			CVN ^b	K _{Jc} ^c	K _{βc} ^d	CVN	K _{Jc} ^a		
Plate HSST-02, C.14% Cu, 0.67% Ni	2.0	31	66	82	70	-15	-5	-50	-23
Weld HSST-68W, 0.04% Cu, 0.13% Ni	1.4	12	11	-6	-2	9	-7	-11	+2
Weld HSST-69W 0.12% Cu, 0.10% Ni	1.2	16	26	46	41	-1	-2	-28	-10
Weld HSST-70W 0.056% Cu, 0.63% Ni	1.7	13	33	23	20	+1	-1	-29	-14
Weld HSST-71W 0.046% Cu, 0.63% Ni	1.7	13	27	-4	12	11	-3	-28	-14

^aIncrease at 200°C.

^bIncrease at 41-J index.

^cIncrease at 125-MPa \sqrt{m} index.

^dIncrease at 90-MPa \sqrt{m} index.

Primarily, the J-integral results have indicated that reduced levels of copper and nickel will reduce the degradation of the upper-shelf tearing modulus. Significant decreases (>25%) in the tearing modulus were observed in all materials with either copper or nickel contents above those of the weld having the lowest levels of these elements. Only when both elements were reduced was the tearing modulus degradation reduced. In terms of initiation fracture toughness, J_{IC} , the upper-shelf level was essentially insensitive to all variables; i.e., radiation, copper content, and nickel content appeared to have little or no effect.

The correlation of the radiation-induced 41-J CVN transition temperature shift with the radiation-induced 125 MPa \sqrt{m} K_{Jc} transition temperature shift is shown in Fig. 9. Note that both mean values and 95% confidence levels are shown in the figure. Welds 69W, 70W and 71W show CVN shifts ranging from 26 to 33°C, while the K_{Jc} shifts range from -4 to 46°C. The 95% confidence limits for these three welds also indicate considerable scatter. For plate 02 and weld 68, the CVN and K_{Jc} transition temperature shifts are fairly close. It is, however, clear that the correlation is only qualitative and the K_{Jc} shift can be nearly 25°C different than the CVN shift.

The correlation of the radiation-induced CVN upper-shelf energy change at 200°C with the radiation-induced K_{Jc} upper-shelf change at 200°C is shown in Fig. 10. Note that both mean and 95% confidence limits are shown. Although the CVN upper-shelf changes range from +10 to -20%, the K_{Jc} upper-shelf changes range from -1 to -7%. For these combinations of copper and nickel, it appears that CVN upper-shelf energy changes do not imply corresponding K_{Jc} upper-shelf changes.

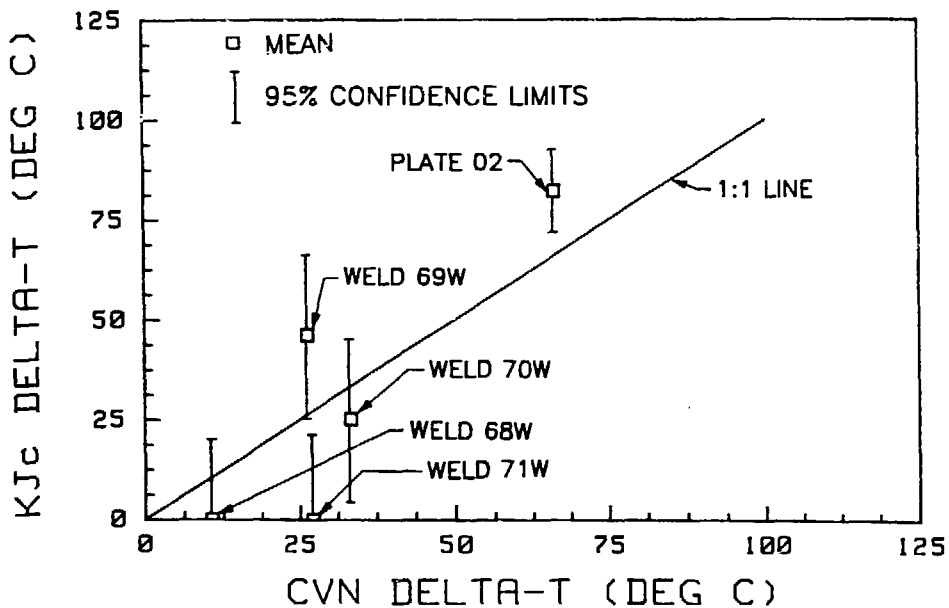


Fig. 9. Correlation of 125 MPa \sqrt{m} K_{Jc} transition temperature with 41-J CVN transition temperature.

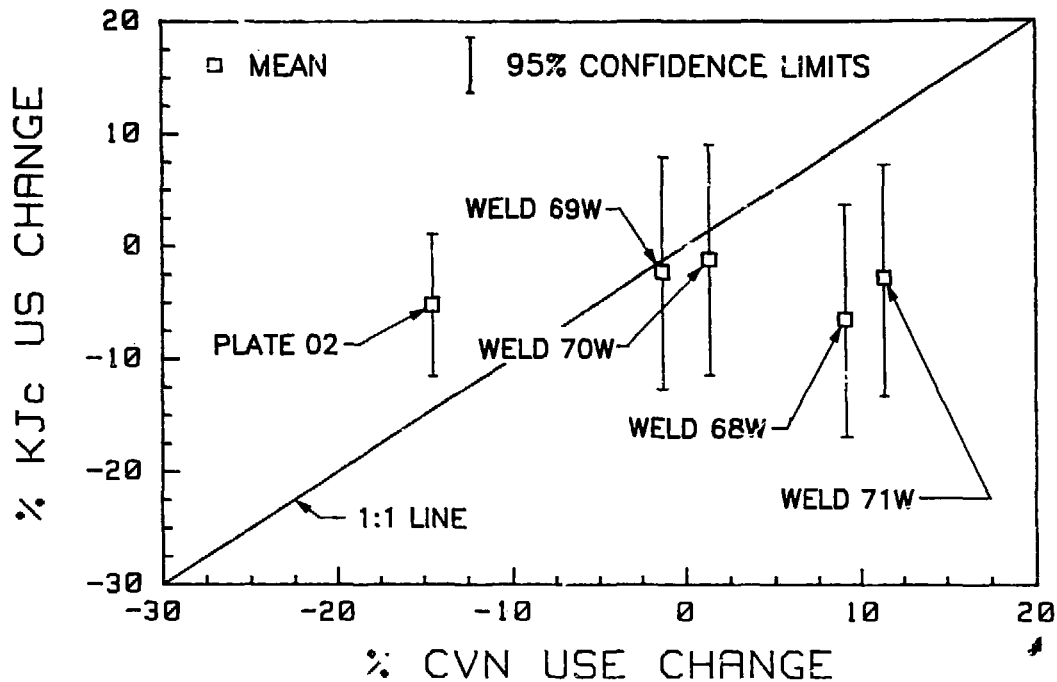


Fig. 10. Correlation of K_{Jc} upper-shelf change with CVN upper-shelf energy change, measured at 200°C.

The correlation of radiation-induced average dJ/da change at 200°C with radiation-induced yield strength change at 200°C is shown in Fig. 11. Note that both mean values and 95% confidence limits are shown. All materials but weld 68W lie close to the 1:1 line indicating a possible correlation. (The large error in weld 68W is a result from large variance in the test data and a small number of specimens available for testing.)

SUMMARY OF OBSERVATIONS FOR FOURTH SERIES

1. There was excellent agreement between the results from the two laboratories, ORNL and MEA (see ref. 26).
2. Upper-shelf elastic-plastic initiation fracture toughness is essentially insensitive to radiation damage for the current production practice welds characterized in this study.
3. Transition temperature shifts to higher temperature with radiation are directly related to the copper and nickel content of the material with copper producing the greatest effect.
4. Upper-shelf initiation fracture toughness and tearing modulus are inversely proportional to temperature.
5. Irradiation degradation in tearing modulus is related to the copper and nickel content of the material.

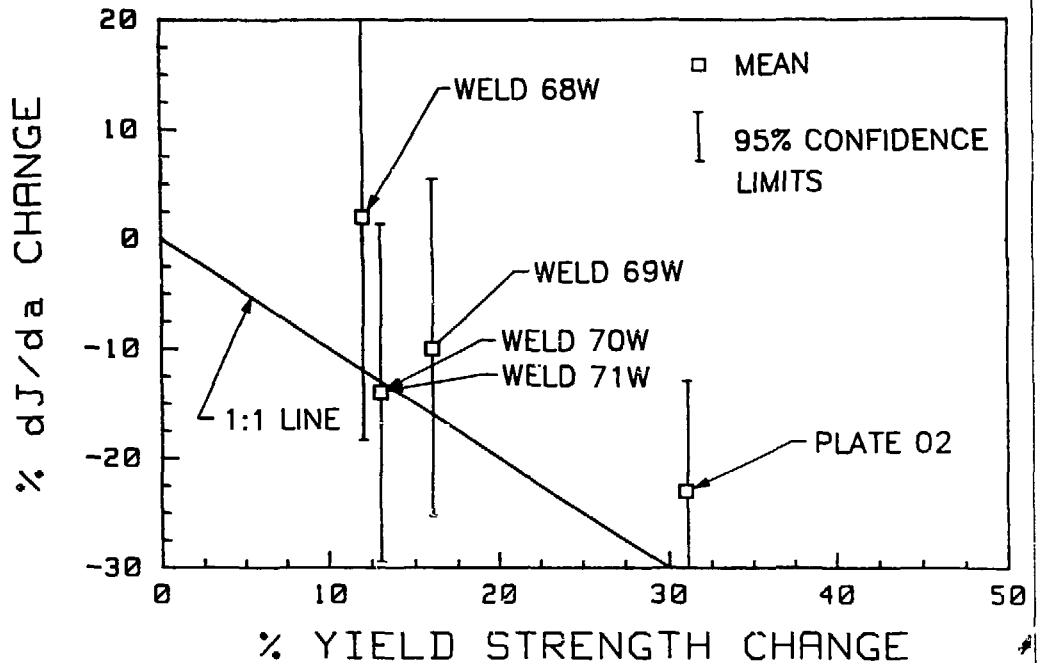


Fig. 11. Correlation of dJ/da change with yield strength change, measured at 200°C.

6. Transition temperature shifts indicated by the CVN data indexed at the 41-J level correlate qualitatively with the fracture toughness data indexed at the 125 MPa \sqrt{m} level for these materials.

7. Upper-shelf energy changes indicated by CVN data correlate poorly with fracture toughness, K_{Jc} , changes.

8. Yield strength changes correlate qualitatively with dJ/da changes.

9. Submerged arc welds with both low copper and nickel contents show essentially zero radiation embrittlement.

FIFTH HSST IRRADIATION SERIES

The primary objective of this program (Fifth HSST Irradiation Series) is to obtain valid fracture toughness (K_{Ic}) curves to as high a level as practical for two nuclear pressure vessel materials irradiated at 288°C.

Currently, estimates of the K_{Ic} curve shift are based on results from Charpy impact testing with the assumptions that the shift of a Charpy toughness curve to higher temperatures can be applied directly to a K_{Ic} curve and that the drop-weight NDT/CVN energy correlation does not change with irradiation. To test these assumptions, this program includes Charpy V-notch impact test specimens and drop-weight test specimens in addition to the compact fracture toughness specimens. Tensile specimens are included in the program to provide data for determining test parameters for the fracture toughness tests and for analysis of the fracture toughness data.

Irradiation and material parameters were chosen to (1) provide significant separation of unirradiated and irradiated properties (i.e., a significant radiation-induced temperature shift of toughness properties); (2) represent, as closely as practical, materials used in early nuclear pressure vessel construction (high copper and nickel contents); and (3) permit program conclusion in a reasonable time period. The chosen irradiation parameters are an irradiation temperature of 288°C (550°F) and a neutron fluence of 1.75×10^{23} neutrons/m² (>1 MeV). The chosen materials are submerged-arc weldments of 0.23 and 0.31% Cu content (0.60% Ni in both weldments). The predicted mean temperature shifts of fracture toughness for these two weldments are 90 and 123°C, respectively, for the above irradiation parameters. These predictions are based on the Metal Properties Council analyses²⁷ of weld metals irradiated in test reactors.

The program plan provides sufficient numbers of specimens to permit meaningful statistical analyses of test results.

MATERIALS

In order to provide as uniform a test material as possible, submerged-arc weldments were fabricated using two special heats of AWS type EF-2 welding wire with copper added in the ladle to achieve the two levels of copper content. One lot, well mixed, of Linde 0124 flux was used for all the welds. The weldments were fabricated and stress-relieved according to commercial practice. The base plate for the weldments is a single 220-mm-thick plate of A-533 grade B class 2 steel. The submerged-arc welding was done by the tandem-arc, alternating-current procedure using a 0° bevel weld groove. The width of the deposited weld metal is about 30 mm. All welds were stress-relieved at 607°C for 40 h. About 14 lin m of each weldment were fabricated for the program. The results of the chemical analysis of the weldments are shown in Table 3.

Table 3. Chemical compositions for welds 72W and 73W

Material	Composition, wt %									
	C	Mn	P	S	Si	Cr	Ni	Mo	Cu	V
72W	0.093	1.60	0.006	0.006	0.44	0.27	0.60	0.58	0.23	0.003
73W	0.098	1.56	0.005	0.005	0.45	0.25	0.60	0.58	0.31	0.003

SPECIMEN COMPLEMENT

The largest practical compact (K_{Ic}) specimen that can be irradiated is a 4TCS specimen. The irradiated yield stress is predicted to be about 620 MPa (90 ksi), resulting in a valid fracture toughness (K_{Ic}) measuring capacity of

130 MPa \sqrt{m} (120 ksi $\sqrt{in.}$). To achieve this toughness level in the unirradiated specimens, having a yield stress of about 480 MPa (70 ksi), requires 8TCS specimens and these are provided for in the program. Smaller fracture toughness specimens are provided for measuring toughness at lower levels, obtaining K_{Jc} values for predicting test parameters for the larger specimens, and obtaining data for comparisons of K_{Ic} and K_{Jc} results. Figure 12 shows the various compact specimens used in this study. A series of irradiation capsules will contain a total of 16 each 4TCS, 36 each 2TCS, 60 each 1TCS, 112 each Charpy-V, 32 each drop-weight, and 28 each subsize tensile specimens, divided equally between the two materials. Sufficient numbers of unirradiated specimens will be tested to provide baseline properties. The numbers of specimens are based on consideration of statistical analysis requirements and the constraints of the irradiation facility. Sufficient weldments are available for fabrication of additional unirradiated specimens, if found necessary.

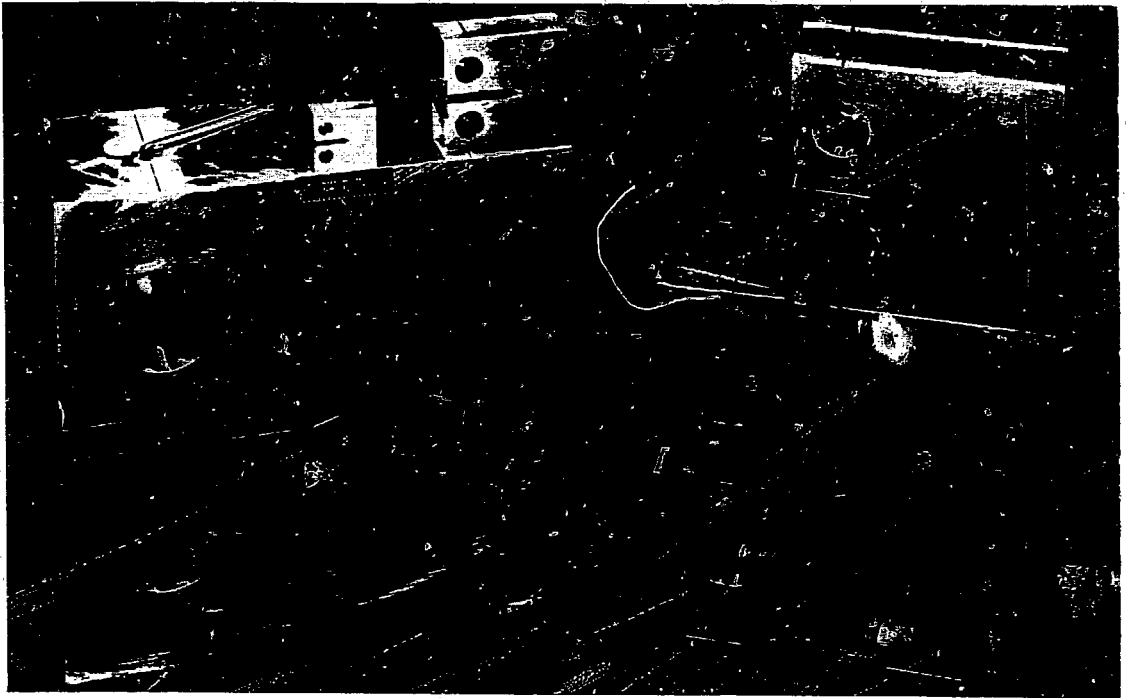


Fig. 12. Compact specimens used in Fifth HSST Irradiation Series. Sizes range from 25 mm thick to 200 mm thick.

IRRADIATION CAPSULE DESIGN AND OPERATION

The Fifth HSST Irradiation Series consists of a total of 12 capsules to be irradiated in the poolside facility of the Oak Ridge Research Reactor (ORR). Neutron dosimetry studies in the facility were conducted in a dummy capsule and a prototype of the 4T capsules was operated in the facility to

obtain neutron and gamma heat parameters for final experiment design. A steel gamma shield was incorporated into the facility to allow control of specimen temperatures. Neutron dosimeter sets are included in each capsule to verify the exposures. An exploded view of a 4TCS capsule and contents is shown in Fig. 13; a similar photograph of a 1TCS and small specimen capsule is shown in Fig. 14.

Specimen temperatures during irradiation were controlled by a combination of electrical heaters and controlled sweep gas composition (helium and nitrogen). The desired 288°C irradiation temperature at the crack front was maintained within 4°C for both the 2TCS and 4TCS specimens. Greater than 90% of Charpy V-notch, tensile and 1TCS test specimens are within 10°C of 288°C. The primary test group of eight drop-weight specimens is $288 \pm 10^\circ\text{C}$, while a second group, to be used for initial scoping studies, is $276 \pm 3^\circ\text{C}$. The neutron fluence (<1 MeV) for the first four 4TCS capsules show an average of 1.78×10^{23} neutrons/m² ($\pm 0.13 \times 10^{23}$ neutrons/m²). Ten of the required 12 capsules have been irradiated with the final two capsules to complete irradiation in early December 1985.

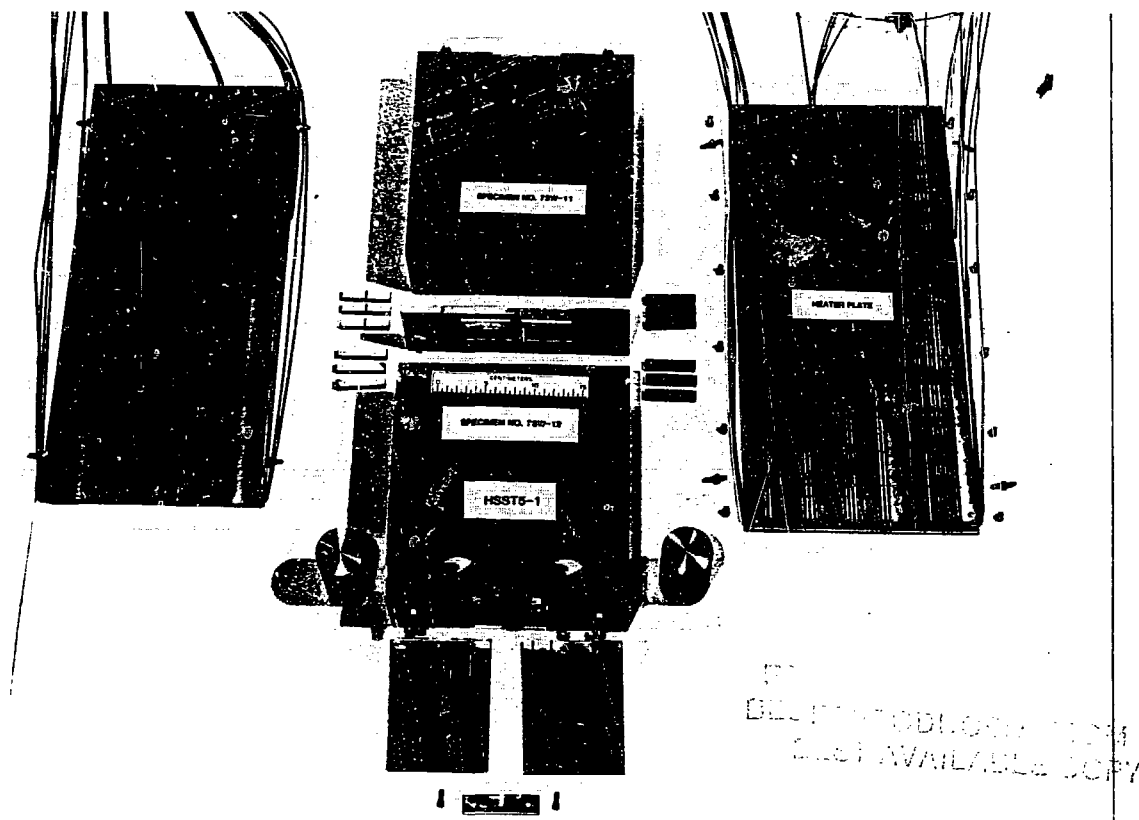


Fig. 13. Exploded view of 4TCS irradiation capsule.

REPRODUCED FROM
BEST AVAILABLE COPY

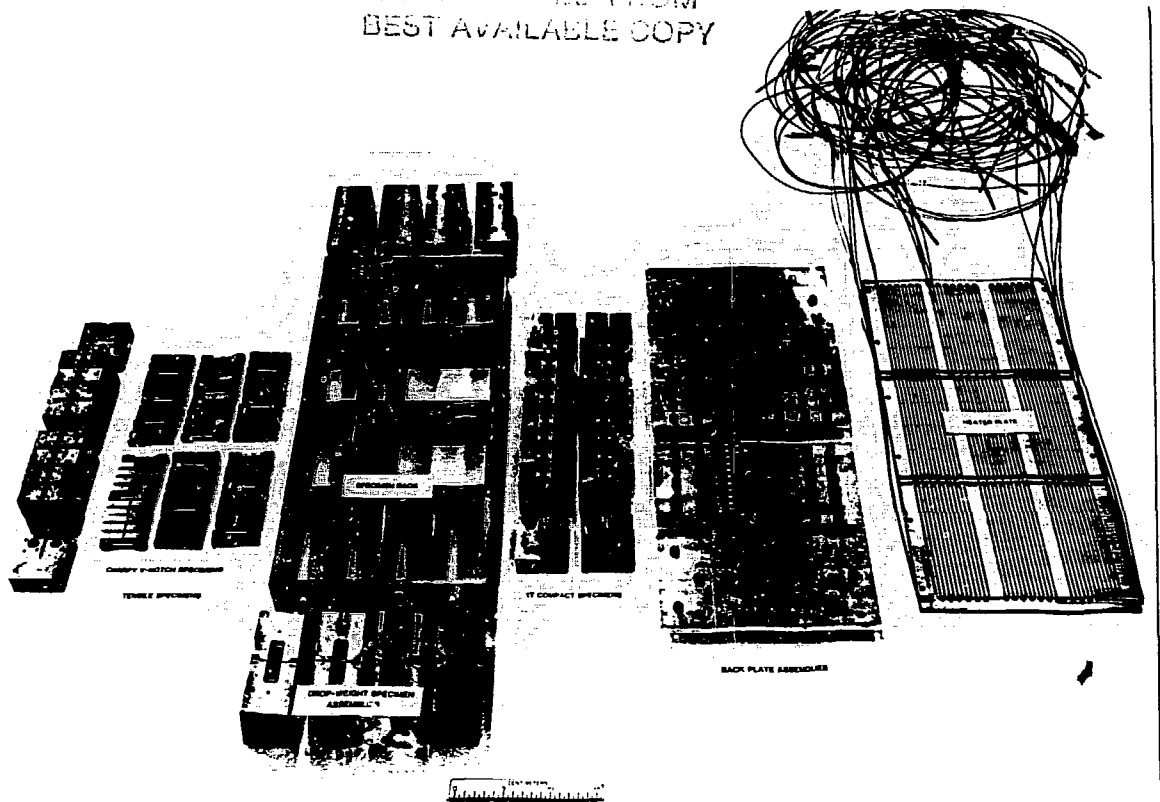


Fig. 14. Exploded view of 1TCS irradiation capsule.

UNIRRADIATED MATERIAL CHARACTERIZATION

The results of tensile tests for welds 72W and 73W are shown in Figs. 15 and 16, respectively. The results of Charpy V-notch tests are shown in Figs. 17 and 18, respectively. A summary of the characterization properties of the two welds is listed in Table 4. Note that the tensile and CVN upper-shelf properties of welds 72W and 73W are very similar; however, weld 73W has a lower transition temperature as measured by drop-weight or CVN tests.

The results of the scoping fracture toughness tests for 1TCS-4TCS specimens for welds 72W and 73W are shown in Figs. 19 through 22. Figures 19 and 20 show the effect of temperature on K_{Jc} for welds 72W and 73W, respectively. Both mean values and ± 1 standard deviation are shown. The scatter for all specimen sizes increases substantially with temperature. The mean values shown for these scoping tests represent multiple testing results (from two to six, depending on the specific case). Figures 21 and 22 show the effect of temperature on $K_{\beta c}$ for welds 72W and 73W, respectively. Note that both mean and ± 1 standard deviation are shown. The scatter for all specimen sizes is substantial. These test results will be used to choose test temperatures for K_{Ic} tests with each material.

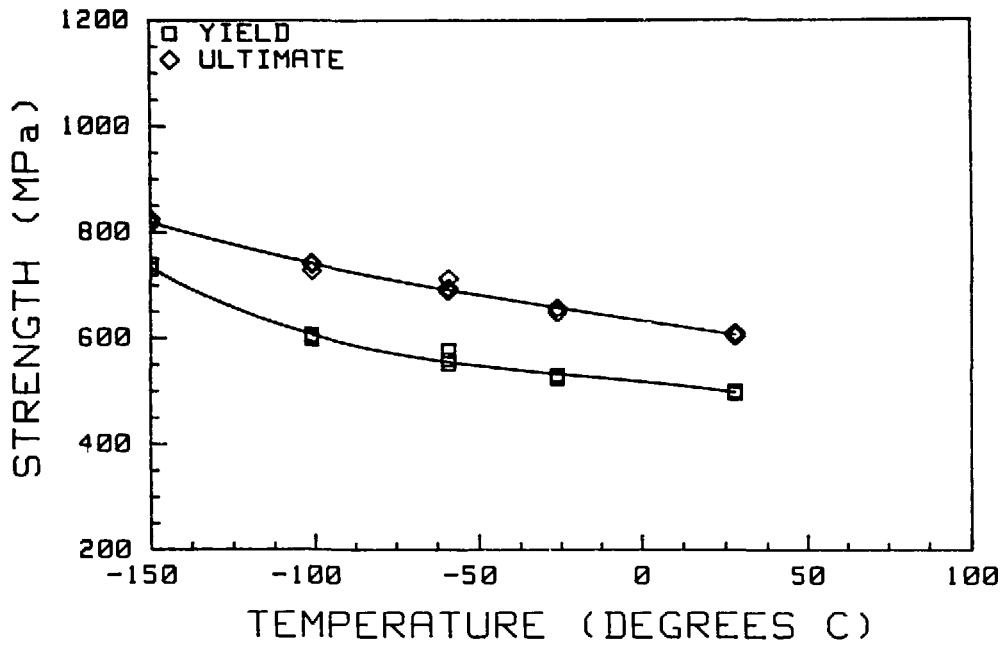


Fig. 15. Variation of yield and ultimate tensile strengths with temperature of HSST weld 72W.

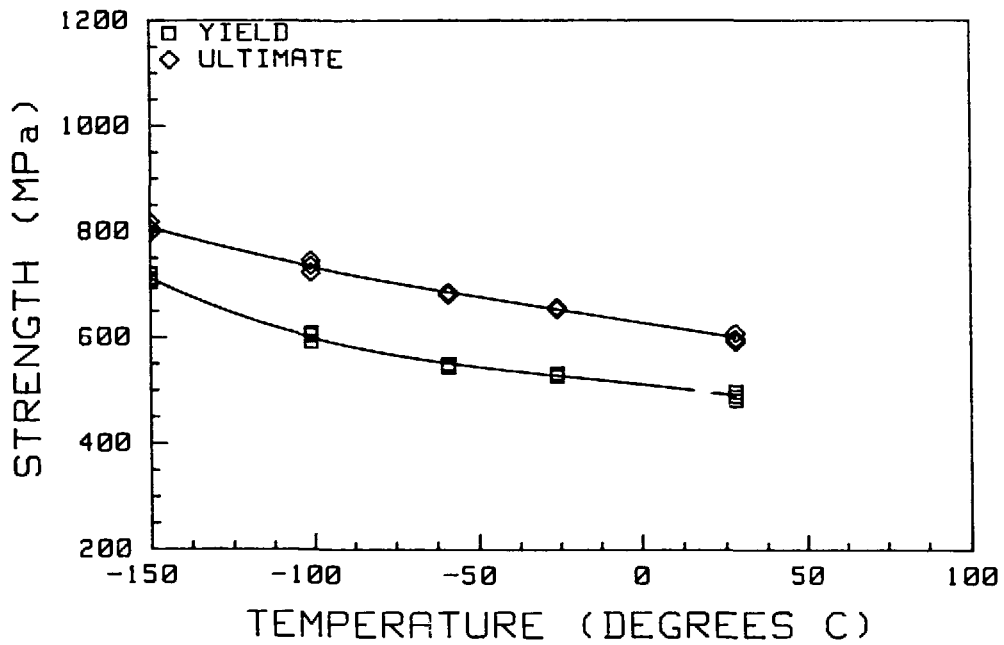


Fig. 16. Variation of yield and ultimate tensile strengths with temperature of HSST weld 73W.

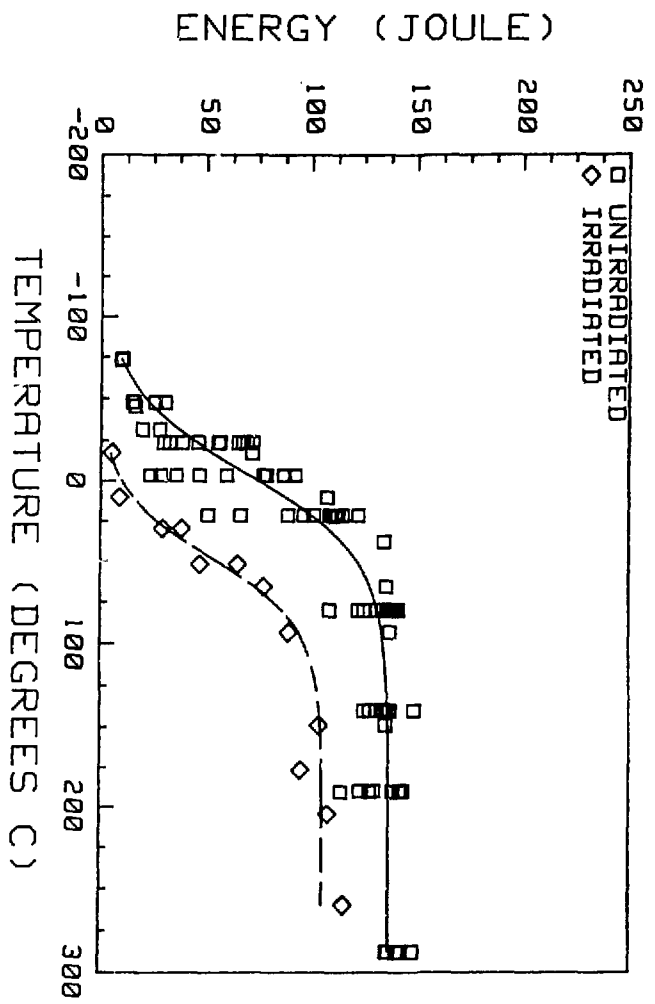


Fig. 17. Variation of Charpy V-notch energy with temperature and irradiation of HSST weld 72W. (Fluence = 1.75×10^{23} n/m², E > 1 MeV.)

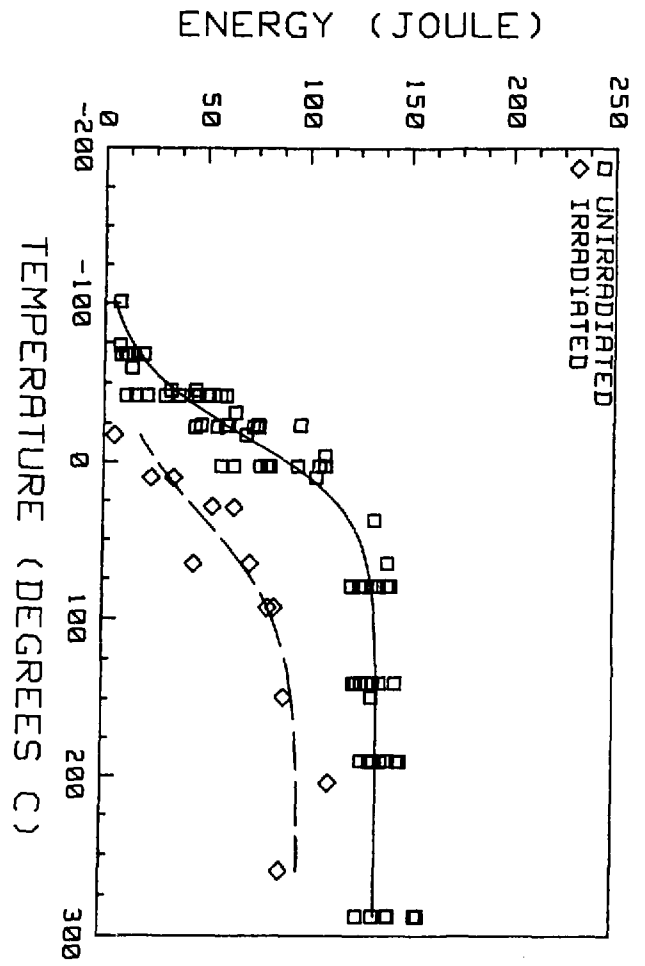


Fig. 18. Variation of Charpy V-notch energy with temperature and irradiation of HSST weld 73W. (Fluence = 1.75×10^{23} n/m², E > 1 MeV.)

Table 4. Summary of mechanical properties for welds 72W and 73W

	Weld 72W	Weld 73W
CVN 41-J transition temperature, °C	-28	-39
CVN fracture appearance (50% shear) transition temperature, °C	-1	-15
Drop-weight nil-ductility temperature, °C	-29	-40
Reference temperature, RT _{NDT} , °C	-29	-40
CVN upper-shelf energy, J	136	135
CVN upper-shelf lateral expansion, mm	2.121	2.084
0.2% offset yield strength at 24°C, MPa	500.3	493.3
Ultimate tensile strength at 24°C, MPa	609.0	603.6 ^d

IRRADIATED MATERIAL CHARACTERIZATION

Preliminary results from Charpy V-notch tests for welds 72W and 73W are shown in Figs. 17 and 18, respectively. The estimated fluence for these specimens is 1.75×10^{23} neutrons/m² (>1 MeV). For weld 72W the irradiation-induced 41-J transition temperature shift is 65°C; and the irradiation-induced upper-shelf drop is 23%. The measured shift is in the range of that estimated before testing (86°C). For weld 73W, the radiation-induced 41-J transition temperature is 64°C; and the radiation-induced upper-shelf drop is 28%. The data scatter is quite high and the measured shift is not close to the estimated shift (121°C). These data are very preliminary in the sense that the data scatter for the unirradiated tests indicate the need for substantially greater numbers of tests to obtain a statistically meaningful determination of the average transition temperature shift. The completion of all unirradiated and irradiated testing for the Fifth Series is currently scheduled for the end of September 1986.

SUMMARY OF OBSERVATIONS FOR FIFTH SERIES

Two submerged-arc welds with different copper contents, but similar in other compositional aspects, have been fabricated for use in investigating the shift and shape of the K_{IC} curve as a consequence of neutron irradiation. Preliminary characterization testing has shown the materials to have similar mechanical properties and fracture behavior. The scatter of toughness results, both CVN and K_{Jc} , however, is relatively high for both materials.

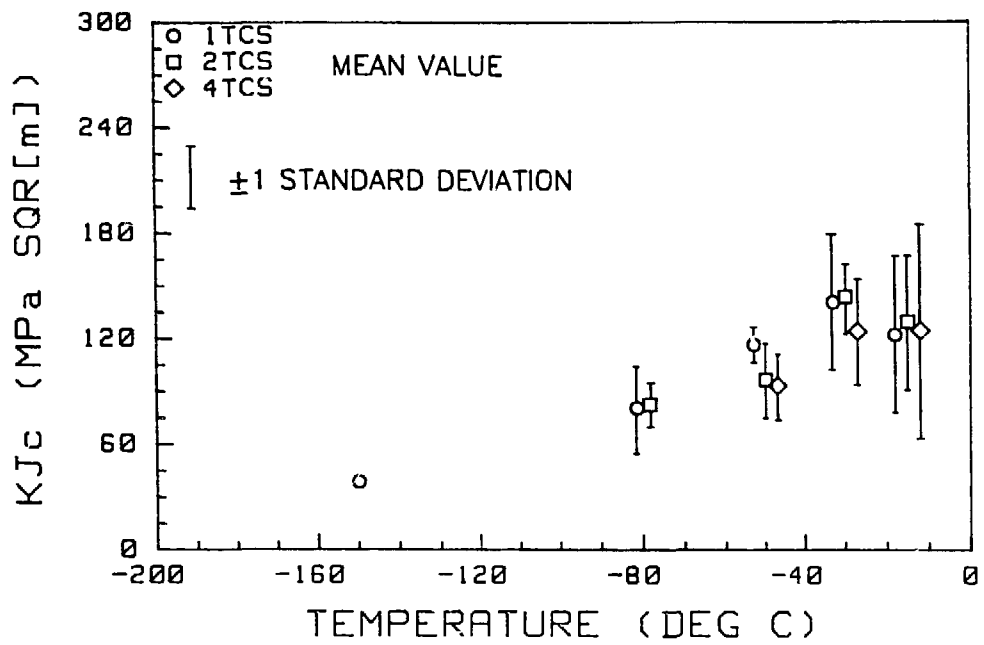


Fig. 19. Variation of K_{Jc} with temperature and specimen size for HSST weld 72W.

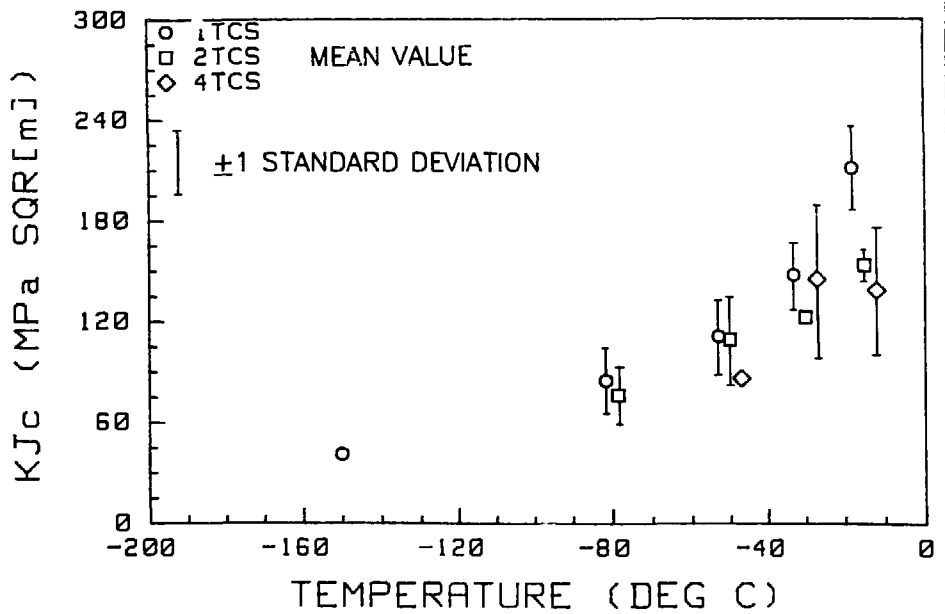


Fig. 20. Variation of K_{Jc} with temperature and specimen size for HSST weld 73W.

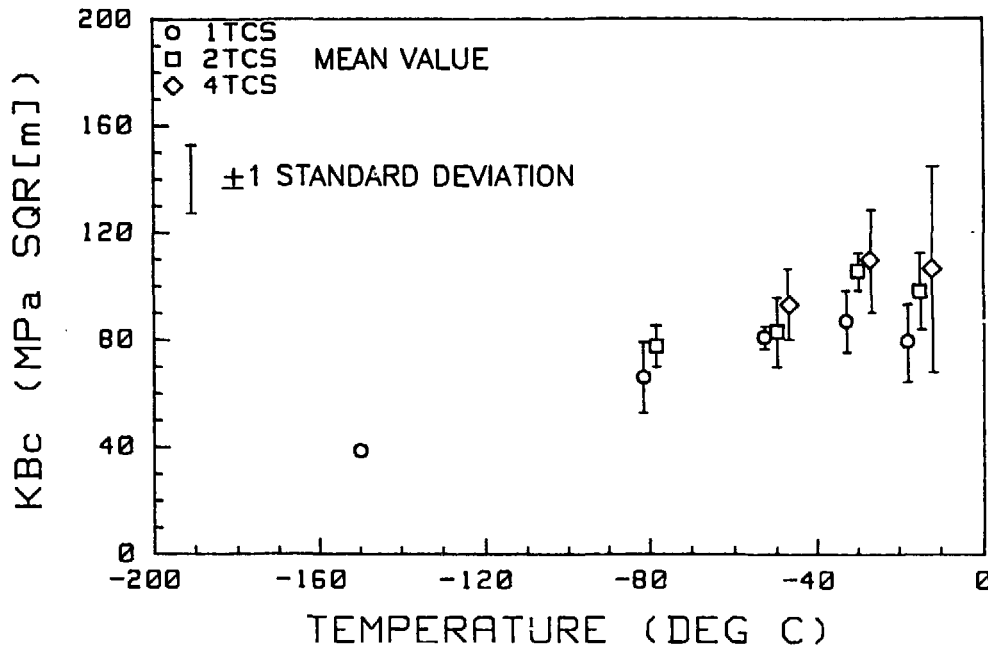


Fig. 21. Variation of $K_{\beta c}$ with temperature and specimen size for HSST weld 72W.

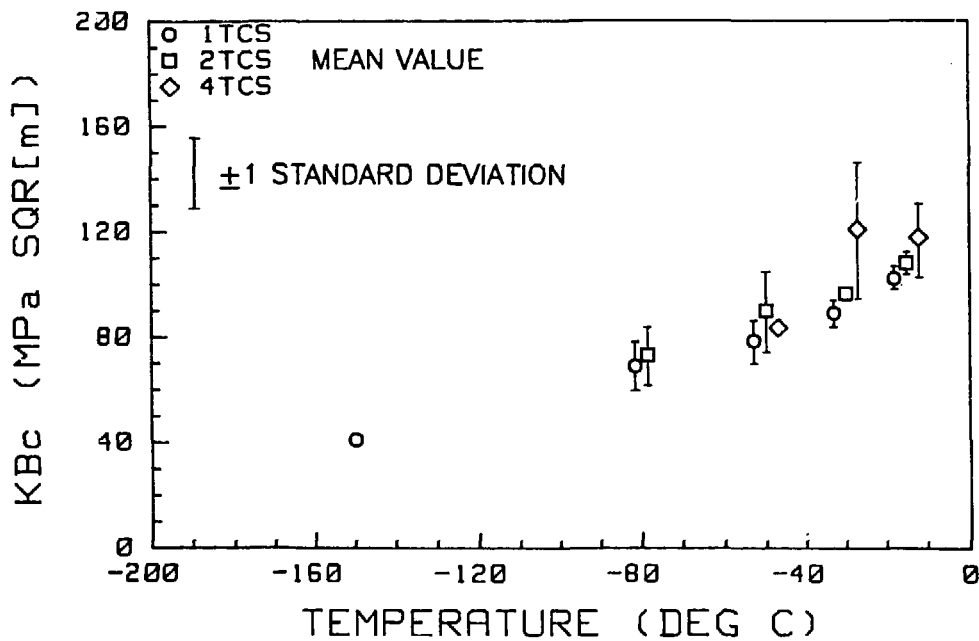


Fig. 22. Variation of $K_{\beta c}$ with temperature and specimen size for HSST weld 73W.

The preliminary CVN tests with irradiated specimens have indicated transition temperature shifts less than those predicted by the MPC method. Only preliminary results have been obtained, however, with testing of additional specimens and statistical analyses yet to be conducted.

ACKNOWLEDGMENTS

We wish to thank M. Vagins of the U.S. Nuclear Regulatory Commission for supporting this study. We appreciate the assistance of the Electric Power Research Institute and Babcock and Wilcox Company in providing the weldments for the Fourth Series. We also wish to thank F. B. Kam and his co-workers for the dosimetry analyses; J. W. Woods and D. Heatherly for construction and operation of the Fourth Series irradiation capsules; T. N. Jones, T. D. Owings, and R. L. Swain for conducting the tests at ORNL; and J. R. Hawthorne, A. Hiser, E. D'Ambrosio, L. Fletcher, and L. Lamont for supervising and/or conducting the tests at MEA. We thank J. L. Bishop and D. L. Northern for preparation of the manuscript.

REFERENCES

1. "Effects of Residual Elements on Predicted Radiation Damage to Reactor Vessel Materials," *Regulatory Guide 1.99* (Rev. 1), U.S. Nuclear Regulatory Commission, Washington, D.C., April 1977.
2. Private communication, P. N. Randall, U.S. Nuclear Regulatory Commission, to R. G. Berggren, Oak Ridge National Laboratory, January 1984.
3. J. D. Varsik and S. T. Byrne, "An Empirical Evaluation of the Irradiation Sensitivity of Reactor Pressure Vessel Materials," pp. 252-66 in *Effects of Radiation on Structural Materials*, ASTM-STP 683, J. A. Sprague and D. Kramer, eds., American Society for Testing and Materials, Philadelphia, 1979.
4. J. F. Perrin, R. A. Wullaert, G. R. Odette, and P. M. Lombrozo, *Physically Based Regression Correlations of Embrittlement Data From Reactor Pressure Vessel Surveillance Programs*, EPRI NP-3319, Electric Power Research Institute, Palo Alto, Calif., January 1984.
5. J. D. Varsik, S. M. Schloss, and J. J. Koziol, *Evaluation of Irradiation Response of Reactor Pressure Vessel Materials*, EPRI NP-2720, Electric Power Research Institute, Palo Alto, Calif., November 1982.
6. G. L. Guthrie, "Development of Trend Curve Formulas Using Surveillance Data-II," pp. HEDL-3-4 in *LWR Pressure Vessel Surveillance Dosimetry Improvement Program, Quarterly Progress Report for the Period April-June 1982*, NUREG/CR-2805, Vol. 2, HEDL-TME-82-19, Hanford Engineering Development Laboratory, Richland, Wash., January 1983.
7. U. Potapovs and J. R. Hawthorne, "The Effect of Residual Elements on the Response of Selected Pressure Vessel Steels and Weldments to Irradiation at 550°F," *Nucl. Appl.* 6(1), 27-46 (1969).

8. C. Guionnet et al., "Radiation Embrittlement of PWR Reactor Vessel Weld Metals: Nickel and Copper Synergism Effects," pp. 392-411 in *Effects of Radiation on Materials*, proceedings of the 11th International Symposium held in Scottsdale, Ariz., on June 28-30, 1982, ASTM STP 782, ed. H. R. Brager and J. S. Perrin, American Society for Testing and Materials, Philadelphia, 1982.
9. C. Leitz et al., "Comparative Irradiation Study of Reactor Pressure Vessel Steel Weld Metals," pp. 412-32 in *Effects of Radiation on Materials*, proceedings of the 11th International Symposium held in Scottsdale, Ariz., on June 28-30, 1982, ASTM STP 782, ed. H. R. Brager and J. S. Perrin, American Society for Testing and Materials, Philadelphia, 1982.
10. C. E. Childress, *Fabrication History of the First Two 12-inch Thick ASTM A533 Grade B, Class 1 Steel Plates of the Heavy Section Steel Technology Program, Documentary Report 1*, ORNL-4313, Oak Ridge National Laboratory, Oak Ridge, Tenn., February 1969.
11. T. V. Marston, M. P. Borden, J. H. Fox, and L. D. Reardon, *Fracture Toughness of Ferritic Materials in Light Water Nuclear Reactor Vessels*, MML-75-152, Combustion Engineering, Inc., Chattanooga, Tenn., October 1975.
12. A. L. Lowe, Jr., and J. I. Quresi, *Fabrication of Weldments Using Linde 80 and Linde 124 Weld Fluxes for HSST-4 Irradiation Program*, BAW-1537, Babcock and Wilcox Company, Lynchburg, Va., June 1981.
13. C. A. Baldwin, *Neutron Spectral Characterization Calculations for the Fourth Nuclear Regulatory Commission Heavy Section Steel Technology IT-CT Irradiation Experiments*, NUREG/CR-3311, ORNL/TM-8782, Oak Ridge National Laboratory, Oak Ridge, Tenn., June 1983.
14. F. W. Stallman, C. A. Baldwin, and F. B. K. Kam, *Neutron Spectral Characterization for the Fourth Nuclear Regulatory Commission Heavy Section Steel Technology IT-CT Irradiation Experiments: Dosimetry and Uncertainty Analysis*, NUREG/CR-3333, ORNL/TM-8789, Oak Ridge National Laboratory, Oak Ridge, Tenn., July 1983.
15. D. Marquardt, "An Algorithm for Least Squares Estimation of Nonlinear Parameters," *J. Soc. Industrial and Appl. Math.* 11(2) (1963).
16. H. A. Ernst, "Material Resistance and Instability Beyond J-Controlled Crack Growth," in *Elastic-Plastic Fracture, Inelastic Crack Analysis*, ASTM STP 803, Vol. 1, ed. C. F. Shih and J. P. Gudas, American Society for Testing and Materials, Philadelphia, 1983, pp. 191-213.
17. P. Albrecht et al., "Tentative Test Procedure for Determining the Plane Strain J_I -R Curve," *J. Test. Eval.* 10(6), 245-51 (November 1982).
18. F. J. Loss, ed., *Structural Integrity of Water Reactor Pressure Boundary Components, Quarterly Progress Report for the Period April-June 1979*, NUREG/CR-0943, NRL Memorandum Report 4064, Naval Research Laboratory, Washington, D.C., Sept. 28, 1979.
19. F. J. Loss, ed., *Structural Integrity of Water Reactor Pressure Boundary Components, Annual Report, Fiscal Year 1979*, NUREG/CR-1128, NRL Memorandum Report 4122, Naval Research Laboratory, Sept. 31, 1979.
20. J. R. Hawthorne, ed., *Evaluation and Prediction of Neutron Embrittlement of Reactor Pressure Vessel Materials*, EPRI NP-2782, Final Report, Electric Power Research Institute, Palo Alto, Calif., December 1982.
21. A. L. Hiser et al., *J-R Curve Characterization of Irradiated Low Upper Shelf Welds*, NUREG/CR-3506, MEA-2028, Materials Engineering Associates, Inc., Lanham, Md., April 1984.
22. G. R. Irwin, "Fracture Mode Transition for a Crack Traversing a Plate," *J. Basic Eng.* 82(2), 417-25 (1960).

23. J. G. Merkle, *An Examination of the Size Effects and Data Scatter Observed in Small-Specimen Cleavage Fracture Toughness Testing*, NUREG/CR-3672, ORNL/TM-9088, Oak Ridge National Laboratory, Oak Ridge, Tenn., April 1984.

24. J. J. McGowan, *Tensile Properties of Irradiated Nuclear Grade Pressure Vessel Plate and Welds for the Fourth HSST Irradiation Series*, NUREG/CR-3978, ORNL-6096, Oak Ridge National Laboratory, Oak Ridge, Tenn., January 1985.

25. R. G. Berggren, J. R. Hawthorne, and R. K. Nanstad, "An Analysis of Charpy V-Notch Impact Toughness of Irradiated A-533 Grade B Class 1 Plate and Four Submerged-Arc Welds," presented at the Twelfth International Symposium on the Effects of Radiation on Materials, Williamsburg, Va., on June 18, 1984, to be published.

26. B. H. Menke, J. J. McGowan, R. G. Berggren, R. K. Nanstad, and K. C. Miller, "Effects of Neutron Irradiation on Fracture Toughness of A-533 Grade B Class 1 Plate and Four Submerged-Arc Welds," presented at the Twelfth International Symposium on the Effects of Radiation on Materials, Williamsburg, Va., on June 18, 1984, to be published.

27. Metal Properties Council Subcommittee 6 on Nuclear Materials, "Prediction of the Shift in the Brittle-Ductile Transition Temperature of Light-Water Reactor (LWR) Pressure Vessel Materials," *J. Test. Eval.* 11(4), 327-60 (July 1983).

DISCLAIMER

This report was prepared as an account of work sponsored by an agency of the United States Government. Neither the United States Government nor any agency thereof, nor any of their employees, makes any warranty, express or implied, or assumes any legal liability or responsibility for the accuracy, completeness, or usefulness of any information, apparatus, product, or process disclosed, or represents that its use would not infringe privately owned rights. Reference herein to any specific commercial product, process, or service by trade name, trademark, manufacturer, or otherwise does not necessarily constitute or imply its endorsement, recommendation, or favoring by the United States Government or any agency thereof. The views and opinions of authors expressed herein do not necessarily state or reflect those of the United States Government or any agency thereof.